Supplementary Figures and Tables

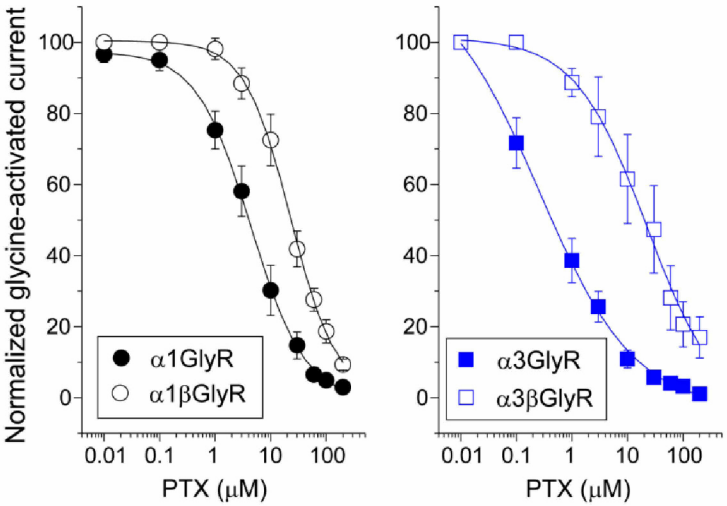

GlyR	IC_{50} (μM)	n_H
α1	4.4±0.2	0.8±0.06
α1β	22.7±1.7*	1.06±0.06
α3	0.26±0.06	0.51±0.04
α3β	22.2±8.0*	0.68±0.12

Figure S1. Picrotoxin sensitivity of recombinant GlyRs. Concentration-response curves of picrotoxin (PTX, 0.01 - 100 μM) were obtained using the EC_{50} of glycine for each GlyR subtype (α1: 45 μM, α3: 200 μM, α1β: 40 μM, α3β: 210 μM). The entire PTX concentration range was tested on each cell. Coexpression of the β subunit significantly reduced picrotoxin sensitivity of α1 and α3 GlyRs, confirming the presence of heteromeric channel complexes containing both α and β subunits. Data are mean ± SEM from 6 - 9 cells per group. *, $p < 0.05$, unpaired t-test.

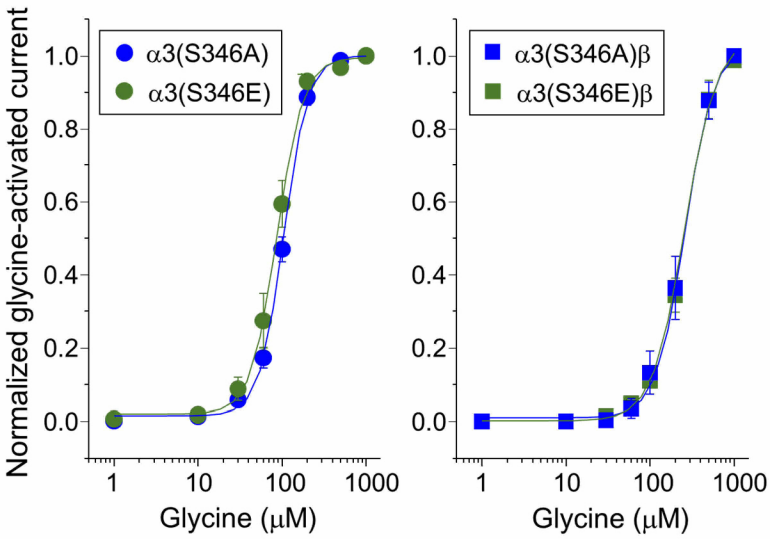

Figure S2. Glycine sensitivity of homomeric and α/β heteromeric α3(S346A) and α3(S346E) point mutated GlyRs expressed in HEK293T cells.

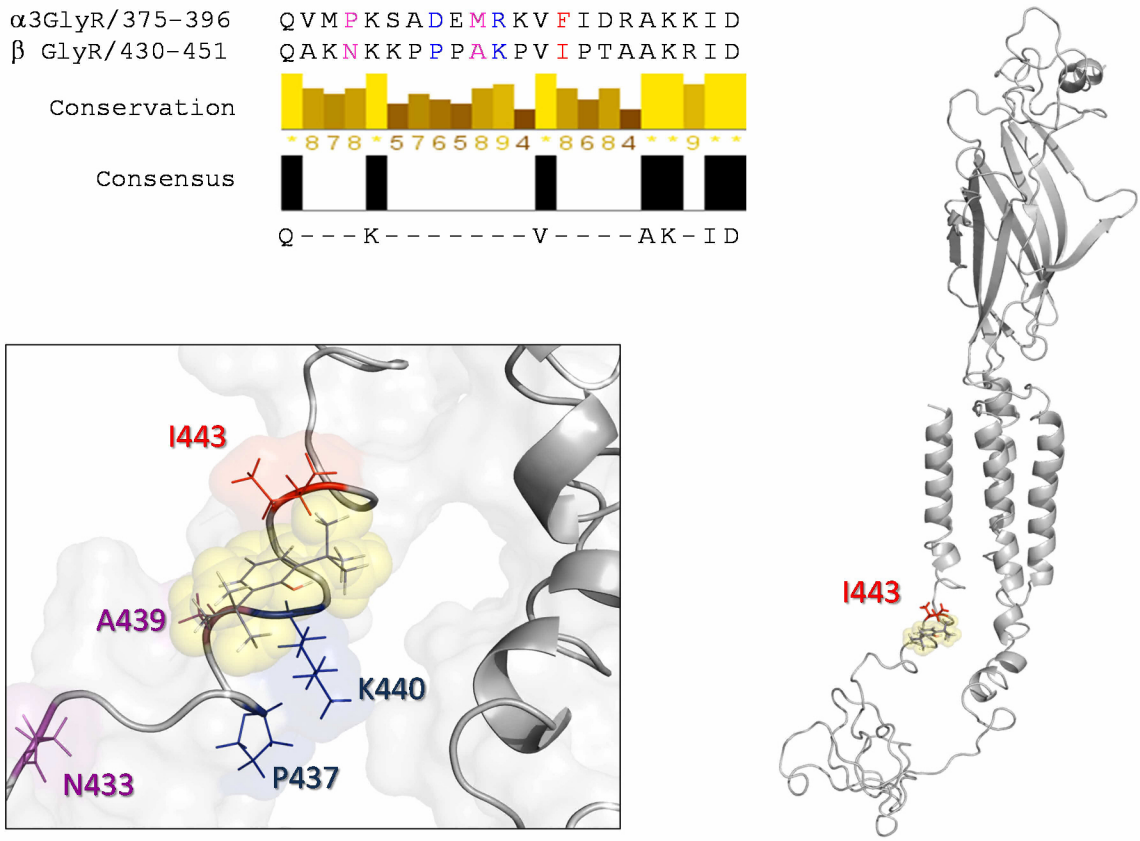

Figure S3. Structural model of GlyR β subunit. (A) Primary sequence alignment of the MA-stretch region of GlyRα3 and GlyR β subunits. The conservation scores are also shown (maximum 11, minimum 1). The identity percentage only reached 32%. **(B)** Homology model of β subunit monomer oriented in the plasma membrane. The location of the I443 residue (which is the counterpart of the F388 in α3GlyR) is highlighted in red. **(C)** Detailed view of the

theoretical acceptor site of 2,6-DTBP in GlyR β

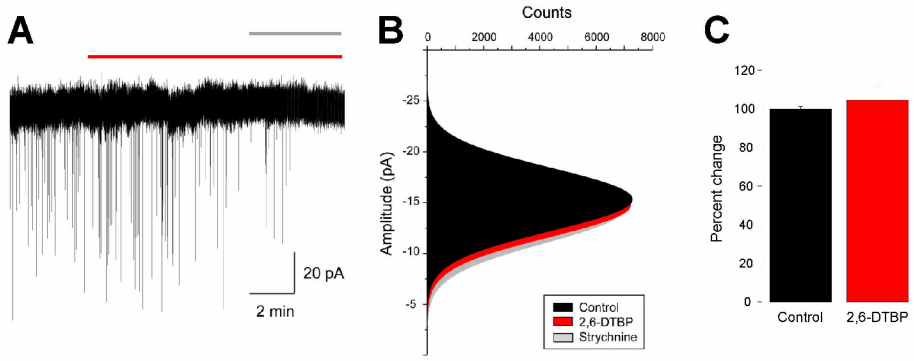

Figure S4. Effects of 2,6-DTBP on tonic glycinergic membrane currents lamina II neurons. Recordings were made in the presence of CNQX (5 µM), D-APV (50 µM) and bicuculline (10 µM). **(A)** Example trace during control conditions, after application of 2,6-DTBP (100 µM) and after additional application of strychnine (1 µM). **(B)** The all-point histograms indicate the holding current amplitudes under these three conditions. **(C)** 2,6-DTBP did not significantly affect the holding current (+4.6 ± 7.6% of control amplitudes, p = 0.56, paired t-test).

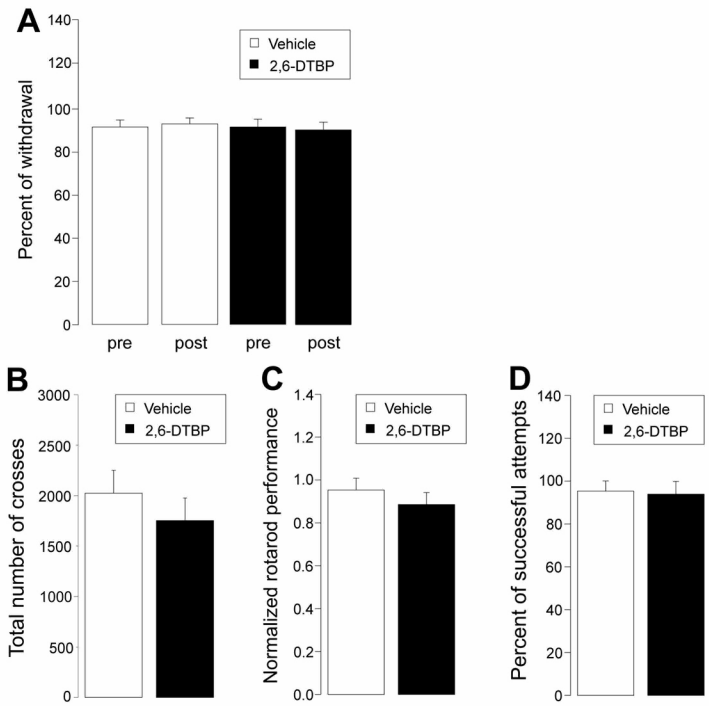

Figure S5. Effects of 2,6-DTBP on locomotor activity, motor coordination, muscle relaxation and acute pain. (A) 2,6-DTBP had no effect on acute nociceptive pain assessed in the pin-prick test in wild-type mice. (**B)** Locomotor activity (number of beam crosses in an open field arena, mean ± SEM) of wild-type mice after the administration of vehicle or 2,6-DTBP. n = 8 mice per group, p = 0.31, unpaired t-test. **(C)** Motor coordination (normalized time spent on an accelerating rotarod, mean ± SEM) of wild-type mice after the administration of vehicle or 2,6-DTBP (n = 7 – 9 mice per group, p = 0.39, unpaired t-test). **(D)** Muscle strength assessed in the horizontal wire test (percent number of successful attempts, mean ± SEM).

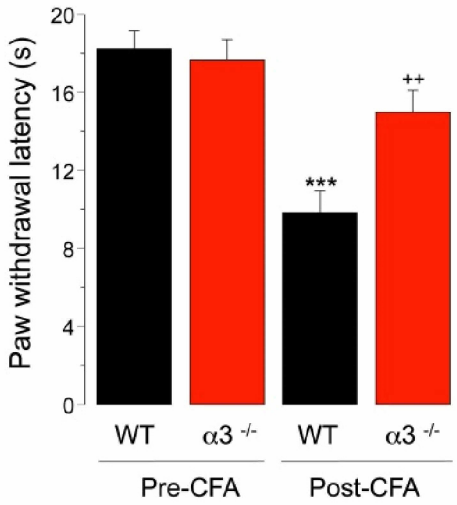

Figure S6. Effects of 2,6-DTBP on heat hyperalgesia in wild-type and in GlyRα3$^{-/-}$ mice after injection of CFA. Paw withdrawal latencies at baseline and 48 hrs after subcutaneous CFA injection. ANOVA followed by Bonferroni post-hoc test. F(3,61) = 10.38. ***, $p < 0.001$ WT pre-CFA versus WT post-CFA, $^{++}$, $p < 0.01$, WT post-CFA versus GlyRα3$^{-/-}$ post-CFA.

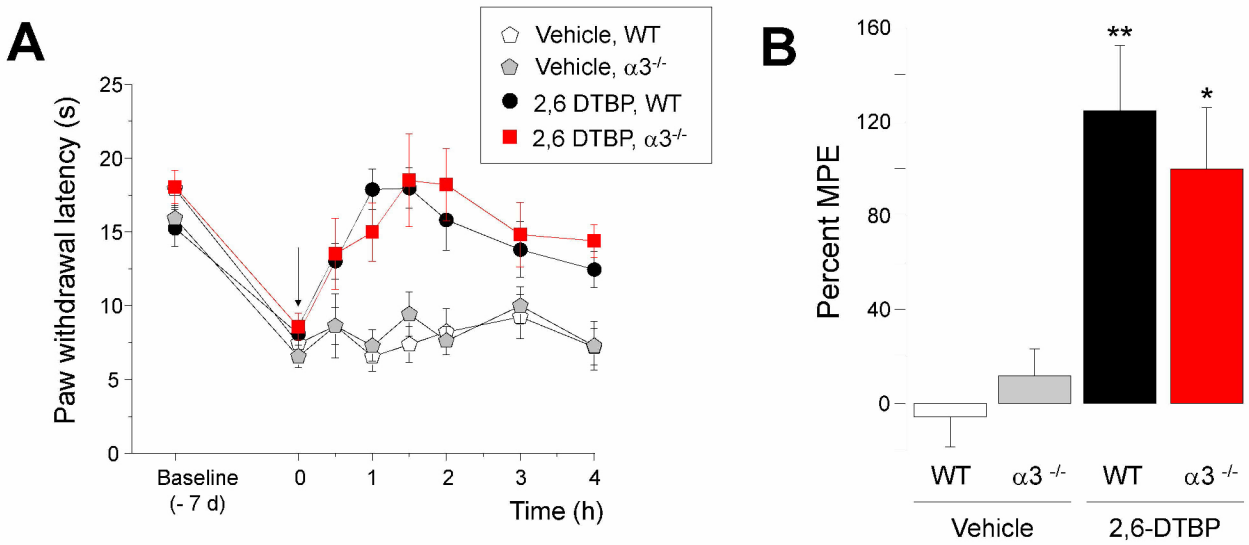

Figure S7. 2,6-DTBP effects on heat hyperalgesia in neuropathic (CCI) wild-type and GlyRα3$^{-/-}$ mice. (A) 2,6-DTBP or vehicle were applied (90 mg/kg, i.p.) on day 7 after CCI surgery. **(B)** ANOVA followed by Bonferroni post hoc test. F(3,25) = 9.42. **, $p < 0.01$, *, $p < 0.05$ before versus after 2,6-DTBP.

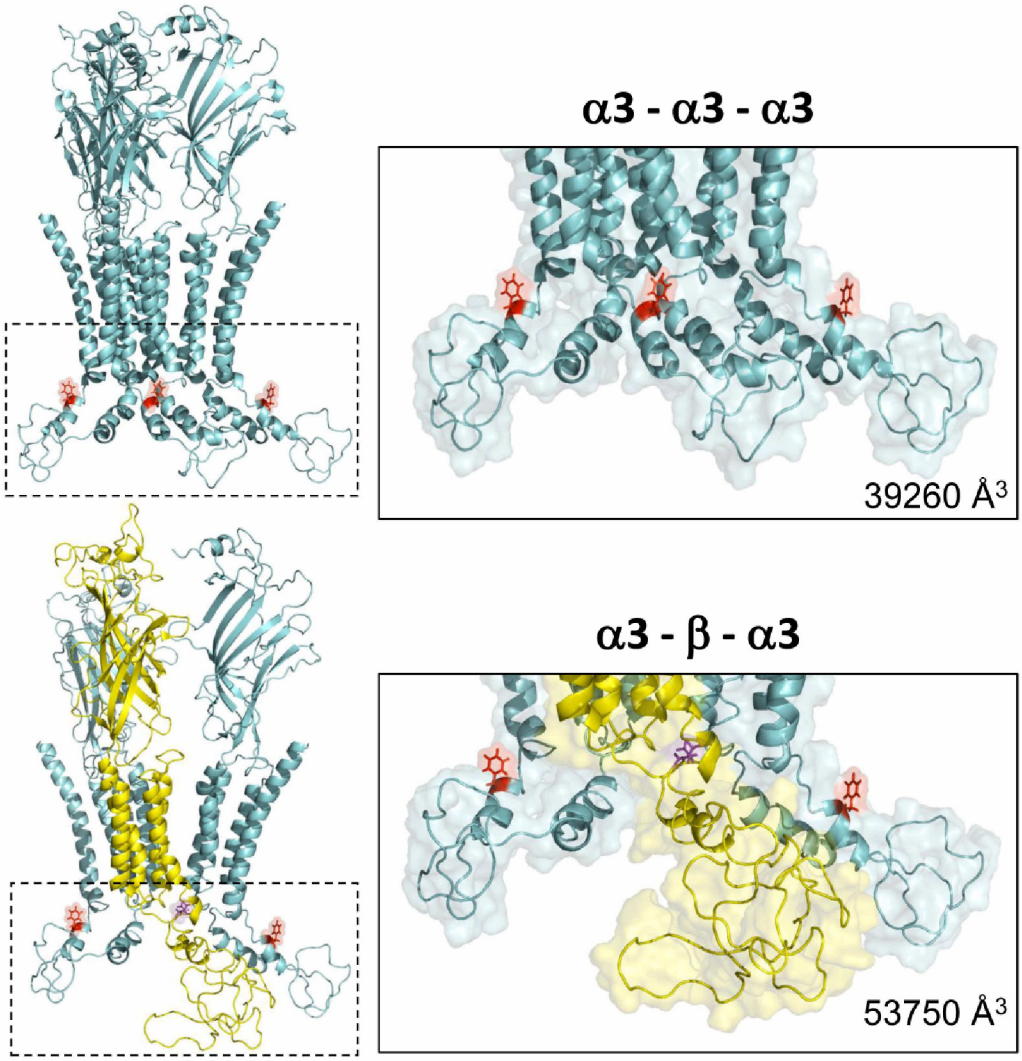

Figure S8. Structural models of the α3-α3-α3 and α3-β–α3 subunit interfaces. Graphic representation of a homotrimeric assembly composed of identical α3 subunits (upper panels, α3 subunits in cyan) and of a heterotrimeric assembly composed by a single β subunit (in yellow) flanked by two α3 subunits (lower panels). Right panels, magnifications of the regions indicated on the left encircling the putative acceptor sites for 2,6-DTBP in the GlyRα3 MA-stretch. The F388 residue in the GlyRα3 subunit and the I443 residue in the GlyR β subunit are highlighted in red and purple, respectively. Calculated volumes of the magnified regions are 39260 Å^3 and 53750 Å^3, for the α3-α3-α3 and the α3-β-α3 assemblies, respectively.

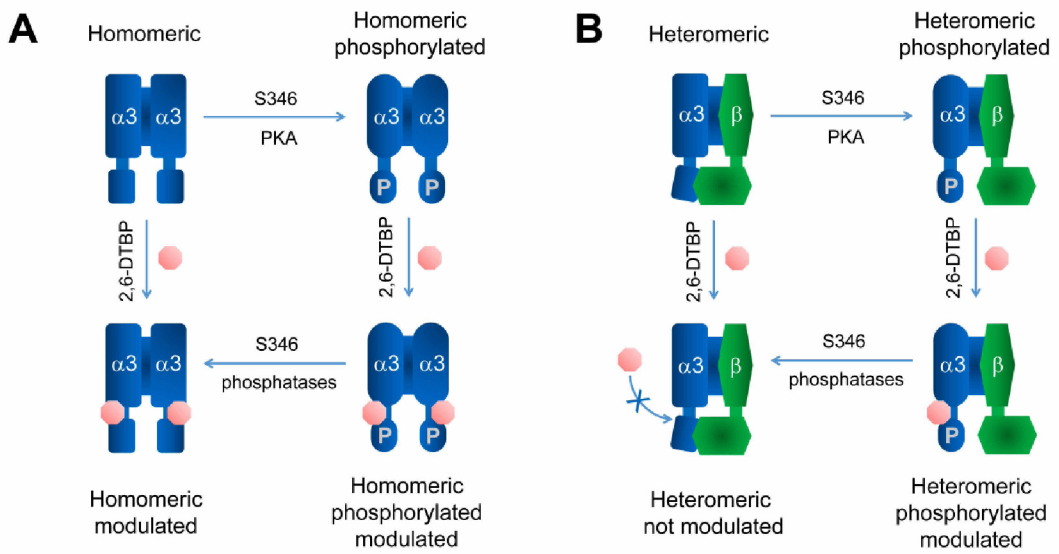

Figure S9. Molecular requirements for allosteric modulation by 2,6-DTBP of α3 and α3β GlyRs with phosphorylated or dephosphorylated GlyRα3 subunits. (A) Dephosphorylated homomeric GlyRα3 are positively modulated by 2,6-DTBP. PKA-dependent phosphorylation of S346 changes the GlyR conformation without preventing the modulation by 2,6-DTBP. **(B)** Heteromeric α3βGlyRs display a low sensitivity to modulation by 2,6-DTBP in their dephosphorylated state possibly due to the occlusion of the 2,6-DTBP interacting site by the β subunit.

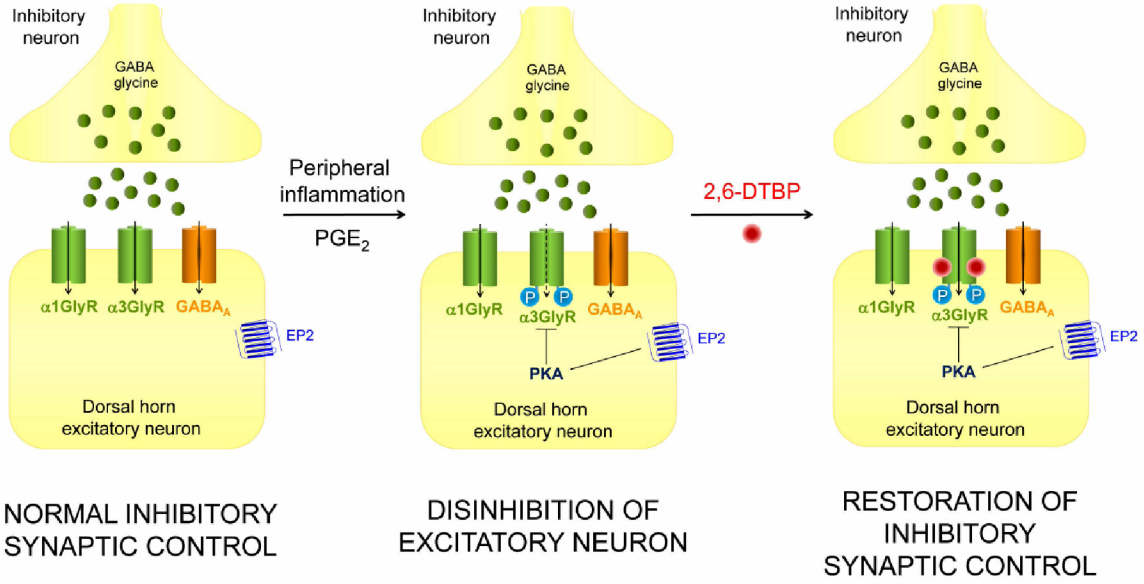

Figure S10. Proposed mechanism of the antihyperalgesic action for 2,6-DTBP. Presynaptic terminals of inhibitory interneurons release the neurotransmitters GABA and glycine into the synaptic cleft, allowing the phasic activation of postsynaptic $GABA_A$ and GlyRs. Under physiological conditions, the chloride influx through these ligand-gated ion channels provides efficient inhibitory control of excitatory neuron activity. Peripheral inflammation stimulates the production of spinal PGE_2, which subsequently activates EP2 receptors and stimulates PKA-dependent phosphorylation of synaptic GlyRs containing $\alpha 3$ subunits. Phosphorylation reduces the inhibitory postsynaptic currents through heteromeric $\alpha 3\beta$GlyRs and disinhibits dorsal horn neurons, which may contribute to the development and maintenance of hyperalgesic states. 2,6-DTBP selectively modulates synaptic $\alpha 3\beta$GlyRs in their phosphorylated states, allowing a restoration of the glycinergic control over the relay of nociceptive signals to higher CNS centers.

Table S1. Concentration-response curves of recombinant GlyRs expressed in HEK293T cells.

	EC_{50} (μM)	n_h	I_{max} (nA)	number of cells
α3	133±15	1.7±0.25	4.3±1.1	8
α1	54±3.0	2.1±0.21	4.2±0.8	9
α3β	117±5.0	3.0±0.32	4.0±1.0	9
α1β	98±4.0	1.9±0.12	4.6±1.0	6
α3 S346A	104±2.1	3.0±0.16	5.7±0.6	18
α3 S346E	101±2.6	2.7±0.17	3.9±0.7	16
α3β S346A	257±10.5	2.3±0.16	3.5±0.5	5
α3β S346E	259±11.0	2.5±0.21	4.3±0.6	5
α3 F388A	79±12.3	1.7±0.27	3.6±0.6	7
α3 S346E-F388A	125±8.1	1.54±0.13	2.9±0.8	3
α3β S346E-F388A	81±6.2	1.7±0.25	4.3±1.2	4

Concentration-response parameters were obtained from fits of normalized current amplitudes to the equation $I_{gly} = I_{max}(gly)n_h/((gly)n_h+(EC_{50})n_h)$. The mean maximal current (I_{max}) indicates the average maximal current elicited by a saturating concentration of glycine (1 mM). Data were calculated from current responses activated by 1, 10, 30, 60, 100, 200, 500, and 1000 μM glycine recorded at a holding potential of -60 mV. All values are mean ± SEM.

Table S2. Single-channel kinetic parameters of wild-type and mutant α3GlyRs in the absence or the presence of 2,6-DTBP.

	GlyRα3							
	Glycine (100 μM)				Glycine (100 μM)/2,6-DTBP (10μM)			
	MOT (ms)	MST (ms)	nPo	Main γ (pS)	MOT (ms)	MST (ms)	nPo	Main γ (pS)
WT	21.6 ±6.0	310.0 ±60.5	0.20 ±0.02	91.0 ±1.20	55.6 ±8.19^{+}	139.2 ±21.5^{+}	0.58 ±0.10^{+}	90.1 ±0.92
F388A	19.1 ±3.2	201.6 ±51.9	0.18 ±0.05	88.2 ±1.82	18.1 ±4.89	213.6 ±27.8	0.19 ±0.04*	88.7 ±1.46

*, p <0.05, t-test, wild-type versus (F388A) point mutated α3GlyR.

$^{+}$, p < 0.05, paired t-test, control condition versus 2,6-DTBP

MOT, mean open time; MST, mean shut time; nPo, open probability; γ, conductance.

Table S3. Binding energy and docking scores of different propofol analogs on α3GlyRs.

	percentage potentiation on α3GlyR	docking score	ΔG binding (kcal/mol)	dock*ΔG index
2,4-di-tert-butylphenol	482±96	-2.79	-40.484	112.950
2,6-di-isopropyl-phenol (propofol)	442±99	-2.505	-38.708	96.962
2,6-di-tert-butylphenol	171±21	-2.133	-42.086	89.784
2,6-di-methoxi-phenol	3.0±20	-2.476	-32.177	79.669

Percent potentiation of wild-type α3GlyRs was calculated from experimental data using a modulator concentration of 100 μM. 2,6-di-methoxi-phenol was inactive on α3GlyRs and showed the lowest Dock*ΔG index. Dock*ΔG reflects the relationship between the docking attributes of each modulator with their binding energy at the respective site. Percent potentiation and the Dock*ΔG index show a linear correlation (r = 0.92, p = 0.08).